

$$F_3 = \frac{1}{2} \left(\frac{\omega}{ck} \right)^4 \left(f_3 - \frac{9}{5} f_5 + \frac{9}{7} f_7 - \frac{1}{3} f_9 \right),$$

$$f_n = (1 + ck/\omega)^{n/2} - (1 - ck/\omega)^{n/2}.$$

A part of the corrections to hydrodynamic equations is thus equivalent to the appearance of dispersion (temporal and spatial) of the kinetic coefficients. In addition, the expressions for the heat flux acquire terms with velocity gradients, and correspondingly terms with temperature gradients appear in the momentum-flux tensor. The value given above for the ratio of the tensors α_{ikl} and β_{ikl} agrees with the principle of symmetry of the kinetic coefficients.

3. The obtained equations can be used to calculate the low-frequency sound dispersion in liquids. From (12) we can readily determine the correction terms for the phase velocity of the sound $c(\omega)$ and for its damping $\Gamma(\omega)$. Without dwelling on the simple calculations, we present the final result:

$$c(\omega) = c - \frac{T}{12\pi\rho c} \left(\frac{\rho\omega}{\gamma} \right)^{3/2} \Phi,$$

$$\Gamma(\omega) = \frac{\gamma\omega^3}{2\rho c^2} \left\{ 1 - \frac{\rho T}{6\pi\gamma^2} \left(\frac{\rho\omega}{\gamma} \right)^{1/2} \Phi \right\},$$

where Φ is a dimensionless quantity equal to

$$\Phi = \frac{211}{1155} + \frac{22}{35} (\varphi - \psi) + (\varphi - \psi)^2 + \frac{11}{35} \frac{c^2}{T} \frac{c_p - c_v}{c_p c_v}$$

$$+ \frac{3}{8} (1 - \psi) \left(\frac{2}{3} - \psi \right) \left(\frac{\gamma}{\eta} \right)^{3/2} - \frac{2}{5\rho c_p} \left(\frac{\partial p}{\partial T} \right)_p \left[\frac{13}{21} + (\varphi - \psi) \right]$$

$$+ \frac{3}{16} \frac{\rho^2 c^2}{T c_p} \left[\rho c_p \frac{\partial}{\partial \sigma} \left(\frac{1}{\rho^2} \frac{\partial \rho}{\partial \sigma} \right)_p - \frac{1}{\rho} \left(\frac{\partial \rho}{\partial \sigma} \right)_p \right] \left(\frac{\gamma c_p}{\kappa} \right)^{3/2} \left(\frac{\partial}{\partial \rho} \frac{c_p}{\rho} \right)_p.$$

The relative corrections to the speed of sound and to the damping are thus proportional respectively to $\omega^{3/2}$ and $\omega^{1/2}$.

I am grateful to E. M. Lifshitz, I. M. Lifshitz, and L. P. Pitaevskii for a useful discussion of the work.

- ¹L. D. Landau and E. M. Lifshitz, *Mekhanika sploshnykh sred* (Mechanics of Continuous Media), Gostekhizdat, Moscow, 1954. [Pergamon, 1958].
- ²D. Burnett, *Proc. Lond. Math. Soc.* **39**, 385 (1935); **40**, 382 (1935).
- ³S. Chapman and T. G. Cowling, *Mathematical Theory of Non-uniform Gases*, Cambridge Univ. Press, 1952.
- ⁴V. S. Galkin, M. N. Kogan, and O. G. Frindlender, *Izv. Akad. Nauk SSSR Ser. Mekh, Zhidkosti i Gaza* No 3, 13 (1970); No. 3, 98 (1971).
- ⁵M. N. Kogan, V. S. Galkin, and O. G. Frindlender, *Usp. Fiz. Nauk* **119**, 111 (1976) [*Sov. Phys. Usp.* **19**, 420 (1976)].
- ⁶A. F. Andreev, *Zh. Eksp. Teor. Fiz.* **59**, 1819 (1970) [*Sov. Phys. JETP* **32**, 987 (1971)].
- ⁷A. F. Andreev and A. E. Meierovich, *Pis'ma Zh. Eksp. Teor. Fiz.* **15**, 56 (1972) [*JETP Lett.* **15**, 39 (1972)].
- ⁸A. F. Andreev and A. E. Meierovich, *Zh. Eksp. Teor. Fiz.* **64**, 1640 (1973) [*Sov. Phys. JETP* **37**, 829 (1973)].
- ⁹L. D. Landau and E. M. Lifshitz, *Zh. Eksp. Teor. Fiz.* **32**, 618 (1957) [*Sov. Phys. JETP* **5**, 512 (1957)].

Translated by J. G. Adashko

Critical phenomena in cholesteric liquid crystals

S. A. Brazovskii and V. M. Filiev

L. D. Landau Theoretical Physics Institute, USSR Academy of Sciences

(Submitted 26 April 1978)

Zh. Eksp. Teor. Fiz. **75**, 1140-1150 (September 1978)

Phase transitions in cholesteric liquid crystals are considered. A phase diagram is derived which makes it possible to explain the existence of intermediate phases in a narrow region between the uniform isotropic (UI) phase and the spiral phase. The critical phenomena are investigated in the light of experiments on the supercooling of the UI phase.

PACS numbers: 64.70.Ew

1. INTRODUCTION

The critical properties of cholesteric liquid crystals (CLC) in phase transitions from the uniform isotropic (UI) phase to the spiral phase have a number of important differences from the critical properties of other systems. A number of experimental^[1-4] and theoretical^[1,5-7] papers have been devoted to the study of the phase transitions in CLC, but some pertinent problems are still far from being completely solved. In particular, the natural supercooling of the UI phase observed in Ref. 4 and the anomalies in the temperature dependence of the pre-critical scattering of light require deeper investigation.

As will be shown below, these anomalies agree qualitatively with the predictions made in Refs. 7 and 8, and with a more complex experimental investigation it ought to be possible to pose the question of the quantitative comparison of the theoretical and experimental results.

The theory developed in Refs. 7 and 8 predicts a discontinuous transition to the spiral phase, occurring in a region of substantial manifestation of critical anomalies due to the effect of critical fluctuations. The alternative is the formation of a planar lattice of spirals, with a triangular structure.^[9] In the experiment of Ref. 4 a discontinuity was observed only in the transition from

the spiral to the UI phase as the temperature was raised to $T_i = 31^\circ\text{C}$, whereas the transition from the UI phase to the spiral phase on lowering of the temperature occurs, with no discontinuity, at the temperature $T_c = 28.5^\circ\text{C}$. It is natural to expect that the temperature T_c is the point of absolute instability, lying in the metastable region $T_c < T_i$. Thus, the phase transition from the UI phase to the spiral phase of the CLC is characterized by two regions of anomalous critical phenomena: $T \approx T_i$ and $T - T_c$.

The theory of the critical phenomena in the region $T \approx T_i$ was developed in Refs. 7 and 8. In the present paper certain results of this theory will be picked out for the purpose of analyzing the existing and prospective experimental investigations. The new result will be the investigation of the system in the vicinity of the absolute-instability point T_c . It will be shown that the cubic anharmonicities of the system, which affect both the short-wavelength modes (corresponding to the spiral structure) and the long-wavelength modes, can be the cause of the second-order phase transition at $T = T_c$. The case when the cubic anharmonicities are always negligibly small, and the system enters the strong-coupling regime as the temperature is lowered, remains unstudied.

2. THE LANDAU THEORY FOR PHASE TRANSITIONS IN CLC

1. The critical properties of a CLC are described by a free-energy functional $F\{\hat{Q}\}$ of the symmetric traceless tensor $Q_{\alpha\beta}(\mathbf{r})$ extracted from the local dielectric-permittivity tensor $\epsilon_{\alpha\beta}(\mathbf{r})$:

$$F\{Q\} = F_0 + T[\mathcal{H}_2\{Q\} + \mathcal{H}_3\{Q\} + \mathcal{H}_4\{Q\}],$$

$$\mathcal{H}_2\{Q\} = \frac{1}{2!} \int d\mathbf{r} [a Q_{\alpha\beta}^2 + b (\partial_\alpha Q_{\beta\gamma})^2 + c \partial_\alpha Q_{\alpha\gamma} \partial_\beta Q_{\beta\gamma} + 2d e_{\alpha\beta\gamma} Q_{\alpha\alpha} \partial_\gamma Q_{\beta\beta}], \quad (1)$$

$$\mathcal{H}_3\{Q\} = \frac{\mu}{3!} \int d\mathbf{r} Q_{\alpha\beta} Q_{\beta\gamma} Q_{\gamma\alpha}, \quad \mathcal{H}_4\{Q\} = \frac{\lambda}{4!} \int d\mathbf{r} (Q_{\alpha\beta})^4$$

where $\partial_\alpha = \partial/\partial r_\alpha$.

The expansion of $\mathcal{H}_2\{\hat{Q}\}$ in normal modes has the form

$$Q_{\alpha\beta}(\mathbf{q}) = \sum_{i=1}^3 \varphi_i^i \sigma_{\alpha\beta}^i(\mathbf{q}), \quad (2)$$

$$\mathcal{H}_2\{Q\} = \frac{1}{2} \sum_{\mathbf{q}, \mathbf{q}'} \tau_i(\mathbf{q}) \varphi_i^i \varphi_i^i, \quad (3)$$

where the tensors $\sigma_{\alpha\beta}^i(\mathbf{q})$ are constructed from the vector $\mathbf{n} = \mathbf{q}/q$ and the vectors \mathbf{l} and \mathbf{l}^* orthogonal to it^[7]:

$$\sigma_{\alpha\beta}^0 = 6^{-1/2} (3n_\alpha n_\beta - \delta_{\alpha\beta}), \quad \sigma_{\alpha\beta}^1 = l_\alpha l_\beta, \quad (4)$$

$$\sigma_{\alpha\beta}^2 = i \cdot 2^{-1/2} (l_\alpha n_\beta - l_\beta n_\alpha), \quad \sigma_{\alpha\beta}^3 = (\sigma_{\alpha\beta}^1)^*, \quad \sigma_{\alpha\beta}^4 = (\sigma_{\alpha\beta}^3)^*.$$

The energies of the normal modes are equal to ($d > 0$)

$$\begin{aligned} \tau^0(q) &= a + (3b + 4c)q^2/3, \\ \tau^{1,2}(q) &= a + bq^2 \mp 2dq = \tau_1 + \Delta_1 (q/q_1 \mp 1)^2, \\ \tau^{3,4}(q) &= a + (b+c)q^2 \mp 2dq = \tau_3 + \Delta_3 (q/q_3 \mp 1)^2. \end{aligned}$$

The lowest extremal energy τ_s is possessed by the mode with the largest extremal wave vector q_s . The free-energy functional (1) admits various stable one-dimensional spiral structures. The ground state of the one-dimensional ordered spiral phase for $\varphi_{3,4} = 0$ is a spiral (the ellipsoid of the permittivity $\epsilon_{\alpha\beta} = \epsilon_0 \delta_{\alpha\beta} + \bar{Q}_{\alpha\beta}$ rotates about the mean axis), and for $\varphi_{1,2} = 0$ is a conical spiral (the mean axis of the ellipsoid is perpendicular to

the axis of the spiral, and the two others have an angle of precession of 45°). In the case of nonzero φ_0 , φ_1 , and φ_3 ($d > 0$) we have a superposition of two spirals with different cholesteric-structure periods. As will be shown below, for $c < 0$ the UI phase can go over to the conical phase.

Assuming that the expansion (1) gives a good description of the properties of the CLC well below the transition point, we obtain for the Frank energy constants: $K_{11} = K_{33}$, $K_{22}/K_{11} = 2b/(2b+c)$. Usually, the relation $K_{22} < K_{11} \approx K_{33}$ is fulfilled, and we may expect that $c > 0$. However, there exist CLC with $K_{22}/K_{33} > 1$ (in Ref. 10, a CLC with $K_{22}/K_{33} \approx 4$ is investigated). It would be interesting to find the region of the conical phase in such CLC. It is necessary, however, to take into account that below the phase-transition point the coefficient ratio b/c depends on the temperature.^[11] Thus, e.g., near the point of the transition from the UI phase to the nematic liquid crystal (NLC) the coefficient c is very small,^[12] but below the phase-transition point the ratio K_{22}/K_{33} in the CLC and in the NLC decreases. Therefore, the existence of a CLC with $K_{22}/K_{33} > 1$ does not in itself imply a negative c . The known optical experiments in CLC give $c > 0$.^[4]

2. We shall investigate the possible phase diagrams of the free-energy functional F . We shall determine the equilibrium value of $Q_{\alpha\beta}(\mathbf{r})$ by substituting the expansions (2) and (3) into the functional (1) and varying with respect to the amplitudes φ_i^i . Owing to the constancy of $Q_{\alpha\beta}^2(\mathbf{r})$ in the spiral structure, higher harmonics with $q/q_s = 2, 3, \dots$ are not generated. Denoting $\varphi_0^0 = \varphi_0$ and $\varphi_{q_s, \mathbf{n}}^s = \varphi_s$, we obtain

$$(F - F_0)/T = \tau_0 \varphi_0^2/2 + (\tau_1 + C_1 \mu \varphi_0) \varphi_1^2 + (\tau_2 + C_2 \mu \varphi_0) \varphi_2^2 + C_0 \mu \varphi_0^2/6 + \lambda (\varphi_0^2 + 2\varphi_1^2 + 2\varphi_2^2)^2/24, \quad (5)$$

where

$$\tau_0 = \tau^0(0) = a, \quad C_0 = \text{Sp}(\sigma_{\alpha\beta}^0)^2, \quad C_s = \sigma_{\alpha\beta}^s \sigma_{\gamma\delta}^s \sigma_{\alpha\gamma}^s \sigma_{\beta\delta}^s,$$

i.e., from (4),

$$C_0 = 1/\sqrt{6}, \quad C_1 = -1/\sqrt{6}, \quad C_2 = 1/2\sqrt{6}.$$

We shall consider the possibility of a phase with non-zero φ_0 , φ_1 , and φ_3 . The conditions for the extremum of the functional (1) determine the quantities φ_0 and φ_3^2 in the following way:

$$\frac{(C_3 - C_1)\mu\varphi_3^2}{3} = \frac{(3C_1 - C_0)\mu\varphi_0^2}{6} + \left(\frac{\tau_1 - \tau_0}{3} + \frac{C_1^2 \mu^2}{\lambda} \right) \varphi_0 + \frac{C_1 \mu \tau_1}{\lambda}, \quad (6)$$

$$\varphi_0 = (\tau_1 - \tau_0)/\mu(C_3 - C_1). \quad (7)$$

Since $C_3 - C_1 > 0$ and $3C_1 - C_0 < 0$, the extremal φ_0 should lie between the roots $x_{1,2}$ of the quadratic polynomial in the right-hand side of the equality (6):

$$x_1 < \varphi_0 < x_2.$$

The value of the free energy at the point of the minimum can be represented as

$$\frac{F - F_0}{T} = \frac{\mu(C_0 - 3C_1)\varphi_0^3}{6} + \left(\tau_0 - \tau_1 - \frac{3C_1^2 \mu}{\lambda} \right) \frac{\varphi_0^2}{2} - \frac{3C_1 \mu \tau_1 \varphi_0}{\lambda} - \frac{3\tau_1^2}{2\lambda}, \quad (8)$$

where φ_0 is determined by the formula (7).

On the other hand, the value of the free energy at the point of the minimum for the spiral phase with $\varphi_{0,1} \neq 0$ is determined by the same equation (8), but the quantity φ_0 is found by minimizing (8) with respect to φ_0 , which leads to the root x_2 of the quadratic polynomial in the

right-hand side of the equality (6). Therefore, the value of the free energy for the phase with nonzero φ_0 , φ_1 and φ_3 is always greater than the value of the free energy for the phase with $\varphi_{0,1} \neq 0$. It is easy to show that the value of the free energy for the phase with nonzero φ_0 and φ_s is always less than the value of the free energy for the phase in which only φ_s is nonzero. Therefore, the phase diagram for the functional (1) is determined by the competition of three phases: $\varphi_{0,1} \neq 0$, $\varphi_{0,3} \neq 0$, and the UI phase.

The values of the free energies of the first two phases can be represented as finite minima of the third-degree polynomials

$$\frac{F_1 - F_0}{T} = \frac{2}{3\sqrt{6}} y_1^3 + \frac{\alpha_1 - 1}{4} y_1^2 + \frac{3\beta_1}{4\sqrt{6}} y_1 - \frac{3\beta_1^2}{32}, \quad (9)$$

$$\frac{F_3 - F_0}{T} = \frac{2}{3\sqrt{6}} y_3^3 + \frac{4\alpha_3 - 1}{4} y_3^2 + \frac{3\beta_3}{4\sqrt{6}} y_3 - \frac{3\beta_3^2}{32}, \quad (10)$$

where

$$\alpha_s = \frac{2\lambda\Delta_s}{\mu^2}, \quad \beta_s = \frac{4\lambda\tau_s}{\mu^2}, \quad y_s = \frac{\lambda\varphi_{0s}}{\mu}, \quad y_s = -\frac{2\lambda\varphi_{0s}}{\mu}. \quad (11)$$

The value of y_s is determined by varying F_s with respect to y_s . Determination of the phase-equilibrium line $F_1 = F_3$ leads to an equation of fifth degree in β_1 . This equation is obtained as the condition for the existence of a common root of the following system of equations:

$$\begin{aligned} & \kappa_1(\theta_3\kappa_3 - \theta_1\kappa_1)y^2 + 20\kappa_1(\theta_1\delta_1 - \theta_3\delta_3 - 2\gamma\eta)y \\ & + 3\kappa_3(\theta_0\theta_3 + 2\delta_3^2\theta_1 - 2\delta_1^2\theta_3) - \theta_1(\theta_1\delta_1 - \theta_3\delta_3 - 2\gamma\eta)^2 = 0, \\ & 2y^2/\sqrt{6} + (\alpha_1 - 1)y/2 + 3\beta_1/4\sqrt{6} = 0, \end{aligned} \quad (12)$$

where

$$\begin{aligned} \kappa_1 &= [(\alpha_1 - 1)^2 - 4\beta_1]/36, \quad \gamma = 2/3\sqrt{6}, \quad \theta_1 = (\alpha_1 - 1)/6, \\ \delta_1 &= \beta_1/4\sqrt{6}, \quad \eta = 3(\alpha_3 - \alpha_1)(\alpha_1 - \alpha_3 + \beta_1)/8, \end{aligned}$$

and κ_3 , θ_3 , and δ_3 are obtained by replacing β_1 by β_3 and α_1 by $4\alpha_3$. Equation (11) is the condition for equality of the extrema of (9) and (10), and Eq. (12) is the extremum condition for (9). Quite apart from the complexity of finding the roots of the system (12), there is the complexity of selecting them correctly: the solutions of the system (12) describe equality of the extrema of F_1 and F_3 , and not just of their minima. Therefore, we shall carry out a qualitative analysis of the possible phase diagrams under the condition of not too large $|c| < b$.

The line of the transition from the UI phase to the spiral phase with $\varphi_{0,1} \neq 0$ is determined by the equation

$$9\beta_1^2 + 2(9\alpha_1 - 1)\beta_1 - 3\alpha_1(1 - \alpha_1)^2 = 0. \quad (13)$$

The analogous transition to the spiral phase with $\varphi_{0,3} \neq 0$ is determined by the equation

$$9\beta_3^2 + 2(36\alpha_3 - 1)\beta_3 - 12\alpha_3(1 - 4\alpha_3)^2 = 0. \quad (14)$$

As we should expect from (9) and (10), in terms of $4\alpha_3$ and β_3 an equation analogous to Eq. (13) is obtained. The lines of transitions from the UI phase to the spiral phases with $\varphi_{0,1} \neq 0$ and $\varphi_{0,3} \neq 0$ for the case $c > 0$ are represented in Fig. 1 by the curves AFL and $ABCD$, respectively. The curve $ABCD$ lies everywhere below the curve AFL . However, this does not guarantee the impossibility of a transition between the two spiral phases of the CLC. The free-energy difference $F_3 - F_1$ can be negative in the region AOB (the y_s that minimizes F_s is always positive; on the line OB , $|\beta_1| = |\beta_3|$). For $c = 0$

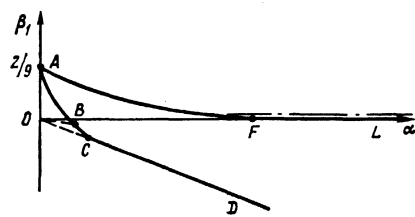


FIG. 1.

and $\alpha_s > 0$ the spiral phase with $\varphi_{0,1} \neq 0$ is the more favorable. In the region AOB the parameter α is small (at the point with $\alpha_1 = (b+c)/4b$). In the leading approximation in small α the difference of the free energies of the phases is determined by the corresponding change in the parameters α and β . The contribution to the free-energy difference from the change in the order parameter is quadratic in α and is not taken into account. Then,

$$\frac{F_3 - F_1}{T} = \frac{c\lambda\alpha^2}{2\mu^2 b(b+c)} \left[\left(\frac{3b}{c} - 1 \right) y^2 + \sqrt{6}y - \frac{3\beta}{2} \right], \quad (15)$$

$$-4y^2 + \sqrt{6}y - 3\beta/2 = 0, \quad (16)$$

where Eq. (16) determines the equilibrium value of the order parameter in the zeroth approximation in α . It is easy to see from Eq. (15) that for $c > 0$ the spiral phase with $\varphi_{0,1} \neq 0$ is always favorable in the region of small α . Therefore, for $0 < c \lesssim b$ the spiral phase with $\varphi_{0,1} \neq 0$ will be realized everywhere below the line AFL .

The phase diagram in the case when the coefficient c is less than zero and small in magnitude is presented in Fig. 2. At the point C , $\alpha_3 = b/(b+c)$, while at the point F we have $\alpha_3 = 1/4$. The shaded region corresponds to the spiral phase with $\varphi_{0,3} \neq 0$. The curves $ABCD$ and AFL are found from the conditions (13) and (14) that the free energies of the spiral phases with $\varphi_{0,1} \neq 0$ and $\varphi_{0,3} \neq 0$, respectively, are equal to zero. It follows from the mutual disposition of the curves that a curve BE separating the two spiral phases should emerge from the point B ; this curve lies everywhere below the curve $ABCD$.

For small $|c|$ the initial segment of the curve BE lies in the region of small $\beta_{1,3}$. In this case, in the expression (10) for F_3 we can neglect the term cubic in φ_3 :

$$(F_3 - F_0)/T \approx -3\alpha_3\beta_3^2/8(4\alpha_3 - 1), \quad \beta_3 \ll 3(4\alpha_3 - 1)^2/2.$$

The expression for F_1 has the form

$$(F_1 - F_0)/T = (\kappa_1 - \theta_1^2)[\theta_1 + \theta_1^2(\theta_1^2 - \kappa_1)]/8\gamma^2 + \kappa_1(\theta_1 - \kappa_1^2)/4\gamma^2.$$

Thus, the curve BE is determined by the equation

$$(F_1 - F_0)/T = -[(\sqrt{6}/\gamma)(\theta_1^2 - \kappa_1) + 12\theta_1 - 3\theta_1^3/2]^2(6\theta_1 + 1)/64\theta_1,$$

while for $\beta_1 \ll 3(\alpha_1 - 1)^2/2$, $\alpha > 1$,

$$\frac{4\alpha_3\beta_3^2}{4\alpha_3 - 1} = \frac{\alpha_1\beta_1^2}{\alpha_1 - 1}.$$

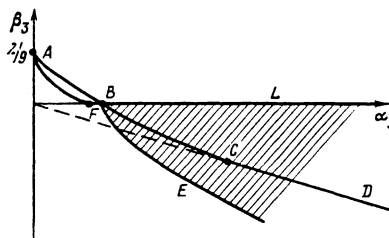


FIG. 2.

It follows from Eqs. (15) and (16) that in the region of small α the spiral phase with $\varphi_{0,1} \neq 0$ is favorable, provided that $c \neq 0$. In the region $|\beta_s| \gg 1$ the difference $F_3 - F_1$ is represented in the form

$$(F_3 - F_1)/T \approx 9|\beta| \alpha / 32,$$

i.e., $F_1 < F_3$ for $\beta_1 \gg 9(\alpha_1 - 1)^2/16$, $\beta_3 \gg 9(4\alpha_3 - 1)^2/16$. The line $\beta \approx 0.05\beta_0$ ($\beta_0 = 2/9$), shown by the dashed-dotted line in Fig. 1, corresponds to the phase transition to a non-unidimensional structure with hexagonal symmetry.^[7] As will be shown below, the cubic vertex for the mode $s = 3$ is equal to zero. Therefore, the nonunidimensional structure does not compete with the phase $\varphi_{0,3} \neq 0$ that we have discovered in the region *LBE*. For $\mu^2 \ll \lambda|\tau|$, non-unidimensional structures become unfavorable.^[8]

3. The parameters of the modes $\tau_s(q)$ can be determined experimentally from the angular dependence of the integrated critical light-scattering intensity

$$I \propto \frac{1}{4} \tau_s^{-1} \sin^2 \varphi + \frac{1}{4} (\tau_s^{-1} + \tau_s^{-1}) \cos^2 \varphi \sin^2 \theta / 2 + \frac{1}{4} (\tau_s^{-1} + \tau_s^{-1}) (1 - \cos^2 \varphi \cos^2 \theta / 2).$$

Here it is assumed that the incident light is polarized at right angles to the scattering plane. The angles between the wave vectors and the polarizations of the incident and scattered light are denoted by θ and φ , respectively.

Experimentally, it is primarily the high-temperature region $T - T_i \approx 10^\circ\text{C}$, in which $\tau_s \gg \Delta_s$, that is investigated. In the zeroth approximation in Δ_s/τ_s , for the scattering intensities I_{VV} and I_{VH} for scattering with $\varphi = 90^\circ$ and $\varphi = 0$ the rule $I_{VH} = 3I_{VV}/4$, characteristic for NLC, is fulfilled. Experimentally, small deviations from this relation are observed in CLC.^[4] They can be used to estimate the coefficient c determining the difference between $\tau_{1,2}$ and $\tau_{3,4}$. In first order in Δ_s/τ_s we obtain

$$1 - 4I_{VH}/3I_{VV} = 4cq^2/3\tau_s.$$

From the data of Ref. 4 we can estimate $cq^2 \approx 0.5^\circ\text{C}$. We note that the size of the low-temperature region of $T - T_c$ amounts to $1 - 3^\circ\text{C}$. Consequently, unlike in Ref. 7, the critical fluctuations of the modes $s = 1$ and $s = 3$ must be treated together when $T - T_c \approx 10^\circ\text{C}$. However, in the limit $T \rightarrow T_c$ the influence of one mode should be decisive.

The rotation of the plane of polarization of light in the high-temperature region enables us to determine only the parameters pertaining to the modes $s = 3$ and $s = 4$.^[7]

3. ANOMALOUS CRITICAL PHENOMENA

1. Depending on the magnitudes of the constants μ and λ in (1), the nonlinearity of the system can be manifested either for $\tau_s > \Delta_s$ or for $\tau_s < \Delta_s$. If in the uniform phase of the CLC we introduce the molecular-orientation correlation length $\xi \approx (b/a)^{1/2}$ characterizing the short-range order akin to that in NLC, then $\tau_s \gg \Delta_s$ corresponds to $2\pi\xi \ll L$, where L is the period of the cholesteric structure. Usually, $\xi \approx 200 - 300 \text{ \AA}$, and for $L \approx 10^4 \text{ \AA}$ the phase transition in a CLC is described by the theory of critical phenomena in NLC.^[13] The limit $2\pi\xi \sim L$ (the point of absolute instability of the UI phase of the CLC, as pointed out by de Gennes^[5]), corresponding to $\tau_s \ll \Delta_s$, was observed in the experiments of Ref. 4 for a CLC with L

$\approx 10^3 \text{ \AA}$ and a large correlation length ξ (because of the proximity to the point of absolute instability of the NLC). The quantity ξ can be estimated if we assume that the correlation length of the mode φ_s , equal to $q_s^{-1}(\Delta_s/\tau_s)^{1/2}$, coincides in order of magnitude with the linear dimensions of the arbitrarily oriented cholesteric domains that were observed below 28.5°C in the experiment of Ref. 4. In the region of temperatures $T < T_{BF}$, where T_{BF} is the temperature at which Bragg peaks appear in the Rayleigh scattering of light at wave vector $2\pi/L$ (Ref. 2), the patterns of the critical phenomena in the NLC and the CLC begin to differ.

Here, as in Ref. 7, we shall consider the second case $\tau_s \ll \Delta_s$. We shall assume that in the region $T \approx T_{BF}$, i.e., $\tau_s \approx \Delta_s$, uniform nematic fluctuations are not yet observed; this leads to the following restrictions on the values of μ and λ :

$$7\lambda q_s^3/12\pi^2 \Delta_s^2 = Q \ll 1, \quad 7\mu^2 q_s^3/48\pi^2 \Delta_s^2 = R \ll 1. \quad (17)$$

The small values of the dimensionless parameters Q and R enable us to give a quantitative description of the critical phenomena. In fact, we shall consider the correlation function of the mode φ_s in the region $\tau_s \ll \Delta_s$ (τ_s is the renormalized value of τ_s):

$$g^s(q) = \langle \varphi_q^+ \varphi_{-q}^- \rangle = [r_s + \Delta_s (q/q_s - 1)^2]^{-1}, \quad (18a)$$

$$g^s(x) = \frac{q_s^3 \sin q_s x}{2\pi (\Delta_s r_s)^{1/2} q_s x} \exp\left\{-xq_s \left(\frac{r_s}{\Delta_s}\right)^{1/2}\right\}. \quad (18b)$$

We shall write down arbitrary diagram for the self-energy part $\Sigma(q_s) = \tau_s - r_s$, in the coordinate representation (18b) for the internal lines. The expressions obtained are found to be insensitive to the presence of the exponential factor in (18b), i.e., the convergence of the integrals is ensured by the oscillatory factors even when the correlation length is infinite. Therefore, we can easily estimate the order of magnitude of an arbitrary diagram containing $2n$ three-point vertices and m four-point vertices:

$$\Sigma_{(m)}^{(2n)} \propto (Q\Delta_s/r_s)^m (R\Delta_s^2/r_s^2)^n (\Delta_s/r_s)^{1/2}. \quad (19)$$

It can be seen from (19) that, for $r_s/\Delta_s \gg Q, R^{2/3}$, we can confine ourselves to the first skeleton diagrams:



$$(20)$$

When lower values of r_s are reached ($r_s/\Delta_s \approx Q$ or $R^{2/3}$), the strong-coupling regime sets in^[8]; this regime will not be considered in the present paper.

2. When all the restrictions indicated above are fulfilled, taking the diagrams (20) into account we obtain the following expression determining the temperature dependence of r_s :

$$\tau_s = r_s + r_{\mu 3}^2/r_s - r_{\lambda 3}^2/r_s^{1/2}, \quad (21)$$

where

$$r_{\mu 3} = \Delta_s (c_{\mu 3} R)^{1/2}, \quad r_{\lambda 3} = \Delta_s (c_{\lambda 3} Q)^{1/2}.$$

The coefficients $c_{\lambda 3}$ and $c_{\mu 3}$ are equal to

$$c_{\lambda 3} = c_{\mu 3} = \pi/5, \quad c_{\mu 1} \approx 2, \quad c_{\mu 3} = 0.$$

Thus, for $s = 3$ we have $r_{\mu 3} = 0$.

For the specific heat we can obtain the expression

$$C = T \left(\frac{\partial \tau_s}{\partial T} \right)^2 \frac{\partial r}{\partial \tau} \frac{q_s^3}{4\pi \Delta_s^{1/2} r_s^{1/2}}. \quad (22)$$

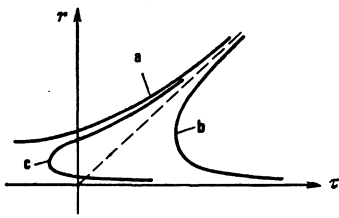


FIG. 3.

The negative corrections to the compressibility and to the energy $a = \tau^s(0)$ of the modes (4) in the long-wavelength limit behave analogously to the specific heat:

$$\frac{\delta a}{a} \propto -r_{\mu}^2 \frac{dr_{\mu}}{d\tau} r_{\mu}^{-\frac{1}{2}} \Delta_s^{-\frac{1}{2}}. \quad (23)$$

A shift also occurs in the observed wave vector:

$$\delta q_1/q_1 \propto (r_1 - \tau_c)^2 \Delta_s^{-\frac{1}{2}} r_{\mu}^{-\frac{1}{2}}. \quad (24)$$

The quantity (24) always remains small.

3. We shall consider the case $s=3$, when $r_{\mu s}=0$. The dependences associated with Eq. (21) were investigated in detail in Refs. 7 and 8. The graph is represented by the curve *a* in Fig. 3. By adjustment of the parameters its shape can be made consistent with the observed^[4] temperature dependence of the linewidth of the scattered light. The expression (22) for the specific heat acquires the form

$$C = T \left(\frac{\partial \tau_3}{\partial T} \right)^2 \frac{q_3^3}{4\pi \Delta_3^{\frac{1}{2}} (r_3^{\frac{1}{2}} + r_{\lambda_3}^{\frac{1}{2}}/2)}.$$

For $r_{\lambda_3} < r_3 < \Delta_s$ the fluctuation correction to the specific heat increases rapidly (approximately like $\tau_3^{-3/2}$), while for $\tau_3 \approx r_3 \approx r_{\lambda_3}$ it approaches saturation.

The dependence analogous to (23) for $\delta a/a$ leads to the shift

$$\frac{\delta a}{a} \propto \frac{R}{Q} \frac{1}{1+2(r/r_{\lambda})^{\frac{1}{2}}}.$$

Substantial softening of the uniform modes can occur only in the case $R < Q$, i.e., on supercooling with respect to the line of orientational phase transitions.^[7] In this region the CLC is close, in its thermodynamic properties, to a NLC, and is, apparently, also incapable of being supercooled. In view of the absence of experimental data we shall not investigate this region. We note only that the softening of the uniform modes saturates at finite values. Further reasons for a first-order phase transition with a volume change can then appear. Returning to the region $R < Q$ under consideration (the principal region of structural phase transitions^[7]), we recall that all the dependences considered are valid in the region $r_{\lambda s} Q^{1/3} < r_s < \Delta_s$, i.e., $-r_{\lambda s} Q^{-1/6} < \tau_s$. At lower temperatures the system is in the strong-coupling regime.

4. We shall consider the case $s=1$, corresponding to the available experimental data.^[2,4] Three regions of parameters are possible.¹⁾

a) If $R \ll Q^{3/2}$, the same dependences occur as for $s=3$.

b) If $R \gg Q^{4/3}$, then $r_{\mu 1} \gg r_{\lambda 1}$ and the term $r_{\lambda 1}$ in (21) is unimportant for all attainable values of r_1 . The formula (21) acquires the form

$$\tau_1 = r_1 + r_{\mu 1}^2/r_1.$$

The curve *b* in Fig. 3 corresponds to this dependence. We see that there appears a critical point $\tau_c = 2r_{\mu 1}$, at which the linewidth (generalized susceptibility) remains finite: $r_c = r_{\mu 1}$. At this point the specific heat and compressibility are singular:

$$C = T \left(\frac{\partial \tau_1}{\partial T} \right)^2 \frac{q_1^2 r_1^{\frac{1}{2}}}{4\pi \Delta_1^{\frac{1}{2}} (r_1^2 - r_{\mu}^2)} \propto (\tau - \tau_c)^{-\frac{1}{2}}.$$

The appearance of the critical point is explained by the dip that appears in the long-wavelength mode $\psi = \phi_1^2$ as a consequence of the attractive interaction via the cubic anharmonicities. Its correlation function $\langle \psi(\mathbf{k})\psi(-\mathbf{k}) \rangle$ is determined by diagrams of the form

$$\text{Diagram 1} + \text{Diagram 2}, \quad \text{Diagram 3} = \text{Diagram 4} + \text{Diagram 5} + \dots \quad (25)$$

The selection of the ladder diagrams is argued in the same way as in Refs. 16 and 8. We obtain

$$D(\mathbf{k}) = \frac{q_1^2}{2\pi r_1^{\frac{1}{2}} \Delta_1^{\frac{1}{2}} (m + (k/q_1)^2 \Delta_1/12r_1)}, \quad (26)$$

for $k/q_1 \ll (r_1/\Delta_1)^{1/2}$ ($m = 1 - r_{\mu 1}^2 r_1^{-2}$), and

$$D(\mathbf{k}) = q_1^2/\Delta_1 r_1 k \quad (27)$$

for

$$(r_1/\Delta_1)^{\frac{1}{2}} \ll k/q_1 \ll 1.$$

As in Ref. 7, the ladder diagrams are summed under the condition $r_{\mu 1}^2 r_1^{-2} \sim 1$. Diagrams with crossed internal lines

$$\text{Diagram 6} \quad (28)$$

have relative order of smallness $(r_1/\Delta_1)^{1/2}$. The point of absolute instability of the metastable phase is determined by $m \rightarrow 0$.

We shall consider the Green function $\langle \phi_1(\mathbf{k})\phi_1(-\mathbf{k}) \rangle$ in the region of small momenta $k \ll q_1$. The diagrams for its self-energy part differ from the diagrams of (25) by the replacement of the end angles by cubic vertices. In this case we obtain

$$g^{-1}(k) = \Delta_1 \left[1 - \frac{2k}{q_1} - \frac{\pi r_{\mu 1}^2 (1 - (k/q_1)^2 \Delta_1/12mr_1)}{28r_1^{\frac{1}{2}} \Delta_1^{\frac{1}{2}} m} \right], \quad (29)$$

where $k/q_1 \ll (r_1 m/\Delta_1)^{1/2}$.

In the region of small momenta

$$k/q_1 \ll (r_1 m/\Delta_1)^{\frac{1}{2}} \quad (30)$$

long before the mode ϕ_1 softens in accordance with formula (29), the three-point and four-point vertices of the modes ϕ_1 , renormalized by fluctuations of the order parameter at momenta $k \approx q_1$, become large. The magnitudes of the vertices are easily estimated:

$$\Gamma_3(k) \approx m^{-3} (r/\Delta)^{\frac{1}{2}}, \quad (31)$$

$$\Gamma_4(k) \approx m^{-5} (r/\Delta)^{\frac{1}{2}}, \quad (32)$$

where k satisfies (30).

The corresponding diagrams have the form

$$\text{Diagram 7} + \text{Diagram 8} \quad (33)$$

Therefore, the formulas (26)–(29) are valid when the cri-

teria (17) are fulfilled for the modes φ_1 in the region of small momenta (30):

$$\Gamma_3^2(r_1 m / \Delta_1)^{1/2} \ll 1, \quad \Gamma_1(r_1 m / \Delta_1)^{1/2} \ll 1. \quad (34)$$

From the formulas (31)–(34) we obtain the condition (27) for neglect of the effect of the strongly interacting long-wavelength excitations on the form of the correlation functions in this region of momenta:

$$m \gg (r_1 / \Delta_1)^{5/9}. \quad (35)$$

From the formulas (26)–(29) it can be seen that the dip in the mode ψ_1 accompanies the dip in the mode φ_1 in the region of momenta (30). Within the limits of the restriction (35), a new stable excitation appears in the correlation function $g_1(k)$ at momenta

$$k/q_1 \ll (r_1 m^4 / \Delta_1)^{1/2}, \quad m \ll 1. \quad (36)$$

In the range of applicability of the criterion (35) the dip in the mode φ_1 is not small.

c) In the intermediate region $Q^{3/2} \ll R \ll Q^{4/3}$ we must use the formulas (21)–(24). In this case, both the regimes (a) and (b) can be observed. In the region $r_1 \gg r_{\mu 1}^4 / r_{\lambda 1}^3$ we can neglect the term with $r_{\mu 1}$ in (21) and we obtain the case (a), or $s=3$. When the value $r_1 = (8/3)^2 r_{\mu 1}^4 / r_{\lambda 1}^3$ is reached the curve bends over. At

$$r_1 = r_{1c} = 2r_{\mu 1}^4 / r_{\lambda 1}^3, \quad \tau_1 = \tau_{1c} = -(1/\sqrt{2} - 1/2) r_{\lambda 1}^3 / r_{\mu 1}^2$$

a critical point analogous to that in case (b) is reached. The dependence (21) corresponds to the curve c in Fig. 3. In the case (c) the formulas (26)–(36) remain valid if

$$m = 1 - r_{\mu 1}^2 r^{-2} + 1/2 r_{\lambda 1}^3 r^{-3/2}.$$

4. CONCLUSION

Investigations of the transitions in CLC from the UI phase to the spiral phase point to the existence of intermediate structures (the so-called "blue" phase) in a narrow range of temperatures.^[14,15] Optical studies reveal the presence in the blue phase of polycrystalline structures—platelets with cholesteric ordering.^[14,15] The color of the platelets is determined by the length of the cholesteric spiral in them. Liquid crystals exist in which the color of the platelets changes strongly—from violet to red—as the temperature is decreased.^[14] It is possible that this can be explained as passage through the

region *LBE* in Fig. 2, since $q_3 > q_1$ (in this case, $c < 0$). We do not know of any restrictions on the sign of the coefficient c . Other liquid crystals display a small change in the color of the platelets.^[15] It is possible then that $c > 0$, and it is necessary to take the non-unidimensional structures into account.^[7,8]

The transition line between the UI phase of the liquid crystal and the hexagonal structure is shown in Fig. 1 by the dashed-dotted line. The dip in the mode φ_1 at the small momenta (30) can turn out to be larger than its dip at $k \approx q_1$ (it is not possible to reach a definite conclusion, since the strong-coupling regime sets in in this region). In this case an intermediate cholesteric structure with a very large (by virtue of the smallness of m) spiral pitch (see (36)) and weak optical activity can appear.

The authors express their gratitude to A. V. Dyugaev and D. E. Khmel'nitskiĭ for useful discussions.

- ¹J. Cheng and R. B. Meyer, Phys. Rev. **A9**, 2744 (1974).
- ²C. C. Yang, Phys. Rev. Lett. **28**, 955 (1972).
- ³D. Coates and G. W. Gray, Phys. Lett. **51A**, 335 (1975).
- ⁴T. Harada and P. P. Crooker, Phys. Rev. Lett. **34**, 1259 (1975).
- ⁵P. G. de Gennes, Mol. Cryst. Liq. Cryst. **12**, 193 (1971).
- ⁶E. I. Kats, Zh. Eksp. Teor. Fiz. **65**, 2487 (1973) [Sov. Phys. JETP **38**, 1242 (1974)].
- ⁷S. A. Brazovskii and S. G. Dmitriev, Zh. Eksp. Teor. Fiz. **69**, 979 (1977) [Sov. Phys. JETP **42**, 497 (1975)].
- ⁸S. A. Brazovskii, Zh. Eksp. Teor. Fiz. **68**, 175 (1975) [Sov. Phys. JETP **41**, 85 (1975)].
- ⁹L. D. Landau and E. M. Lifshitz, Statisticheskaya fizika (Statistical Physics), "Nauka", M., 1964 (Engl. transl. published by Pergamon Press, Oxford, 1969).
- ¹⁰H. Baessler and M. M. Labes, J. Chem. Phys. **51**, 1846 (1969).
- ¹¹I. Haller and J. D. Litster, Phys. Rev. Lett. **25**, 1550 (1970).
- ¹²B. Chu, C. S. Bak, and F. L. Lin, Phys. Rev. Lett. **28**, 1111 (1972).
- ¹³P. B. Vigman, A. I. Larkin, and V. M. Filev, Zh. Eksp. Teor. Fiz. **68**, 1883 (1975) [Sov. Phys. JETP **41**, 944 (1975)].
- ¹⁴W. Elser, J. L. W. Pohlmann, and P. R. Boyd, Mol. Cryst. Liq. Cryst. **20**, 77 (1973).
- ¹⁵D. Coates, K. J. Harrison, and G. W. Gray, Mol. Cryst. Liq. Cryst. **22**, 99 (1973).
- ¹⁶Yu. A. Nepomnyashchii and V. A. Podol'skiĭ, Zh. Eksp. Teor. Fiz. **69**, 555 (1975) [Sov. Phys. JETP **42**, 283 (1975)].

Translated by P. J. Shepherd